Chinese Chemical Letters 32 (2021) 830–833

Contents lists available at ScienceDirect

Chinese Chemical Letters

journal homepage: www.elsevier.com/locate/cclet

Communication

Cobalt and nitrogen atoms co-doped porous carbon for advanced electrical double-layer capacitors

Aiqin Xiang[a], Shuai Xie[b], Fei Pan[c], Hongchang Jin[b], Yiheng Zhai[a], Yanwu Zhu[c], Xianghua Kong[a,d,*], Hengxing Ji[b,**]

[a] School of Chemistry and Chemical Engineering, Hefei University of Technology, Hefei 230009, China
[b] Hefei National Laboratory for Physical Sciences at the Microscale, CAS Key Laboratory of Materials for Energy Conversion, Department of Applied Chemistry, University of Science and Technology of China, Hefei 230026, China
[c] Hefei National Laboratory for Physical Sciences at the Microscale, CAS Key Laboratory of Materials for Energy Conversion, Department of Materials Science and Engineering, University of Science and Technology of China, Hefei 230026, China
[d] CAS Key Laboratory of Materials for Energy Conversion, Hefei 230026, China

ARTICLE INFO

Article history:
Received 17 February 2020
Received in revised form 19 April 2020
Accepted 30 April 2020
Available online 11 May 2020

Keywords:
Electrical double-layer capacitors
Cobalt atoms
Pyridinic nitrogen
Co-doped
Density of states

ABSTRACT

Electrical double-layer capacitors are widely concerned for their high power density, long cycling life and high cycling efficiency. However, their wide application is limited by their low energy density. In this study, we propose a simple yet environmental friendly method to synthesize cobalt and nitrogen atoms co-doped porous carbon (CoAT-NC) material. Cobalt atoms connected with primarily pyridinic nitrogen atoms can be uniformly dispersed in the amorphous carbon matrix, which is benefit for improving electrical conductivity and density of states of the carbon material. Therefore, an enhanced performance is expected when CoAT-NC is served as electrode in a supercapacitor device. CoAT-NC displays a good gravimetric capacitance of 160 F/g at 0.5 A/g combing with outstanding capacitance retention of 90% at an extremely high current density of 100 A/g in acid electrolyte. Furthermore, a good energy density of 30 Wh/kg can be obtained in the organic electrolyte.

Electrical double-layer (EDL) capacitors store energy through the formation of EDL at a porous electrode surface, which is a promising energy storage device when high power density, long cycling life, and cycling efficiency is required [1,2]. However, the typical cell-level energy density of a commercial supercapacitor is at the range of 10–20 Wh/kg, which is less than 10% of commercial Li-ion batteries [3–5]. Therefore, research has focused on increasing the energy density of supercapacitor without sacrificing the power and cycling life. Two major strategies are proposed and studied, which are developing electrolytes of wide electrochemical potential windows since the energy density is proportional to the square of cell voltage [6,7], and optimizing electrode materials since at a given maximum voltage the energy density is proportional to the electrode capacitance [8,9].

An electrode of excellent electrical conductance, large surface area, and suitable structure are critical to yield a large gravimetric capacitance [10–14]. For example, Zhu *et al.* [15] prepared the activated microwave exfoliated graphite oxide (a-MEGO) with an abundant nanopores and a large specific surface area (SSA) of up to 3100 m^2/g using chemical activation method. They found that the gravimetric capacitance of the a-MEGO was as high as 166 F/g and the energy density was up to 70 Wh/kg in the 1-butyl-3-methyl-imidazolium tetrafluoroborate (BMIM BF_4)/AN electrolyte. Chmiola *et al.* [16]. studied the effect of pore size on the gravimetric capacitance using carbide-derived carbons (CDCs) with controlled pore sizes in the range of 0.6–2.25 nm, and found that CDCs with a pore diameter of less than 1 nm showed abnormally large capacitance and was inversely proportional to the micropore diameter. These two works demonstrate that a carbon material of high SSA with suitable porous structure is critical to yield an advanced capacitance for energy storage. Besides the structure of the carbon materials, our previous studies highlight the critical role of the electronic structure of carbon materials on the EDL capacitance, in which we demonstrated that the low density of states (DOS) near the Fermi level renders a quantum capacitance lower than the EDL capacitance, thus limiting the gravimetric capacitance of the electrode [8]. Heteroatoms doping and topologic defects can shift the Fermi level and

* Corresponding author at: School of Chemistry and Chemical Engineering, Hefei University of Technology, Hefei 230009, China.
** Corresponding author.
E-mail addresses: kongxh@hfut.edu.cn (X. Kong), jihengx@ustc.edu.cn (H. Ji).

https://doi.org/10.1016/j.cclet.2020.04.058
1001-8417/

increase the DOS, respectively, both of which improve the gravimetric capacitance [17]. Therefore, tuning the electronic structure of carbon electrode materials through heteroatom doping is a promising strategy to improve the gravimetric capacitance of a carbon electrode.

In this work, we propose a simple yet environmental friendly method to synthesize cobalt and nitrogen atoms co-doped porous carbon (CoAT-NC) material. Our previous research indicates that the Co-N moieties embedded in graphene lattice considerably increase the DOS of graphene at the Fermi-level [18], therefore an improved gravimetric capacitance and capacitance retention at high current densities are expected when the CoAT-NC is served as the electrode material. The CoAT-NC contains Co-N moieties with Co atom concentration of 0.14 at% that can deliver a gravimetric capacitance of 160 F/g at current density of 0.5 A/g. Notably, a gravimetric capacitance of 144 F/g, corresponding to a capacitance retention of 90%, can be preserved at a high current density of 100 A/g when measured in 1 mol/L H_2SO_4 aqueous electrolyte. A high capacitance retention is also observed using 6 mol/L KOH aqueous electrolyte, and a good energy density of 30 Wh/kg is achieved using organic based electrolyte.

D(+)-Glucose monohydrate ($C_6H_{12}O_6{\cdot}H_2O$), sodium chloride (NaCl), and cobalt(II) chloride hexahydrate ($CoCl_2{\cdot}6H_2O$) were purchased from Sinopharm Chemical Reagent Co., Ltd. The synthesis process is illustrated in Fig. 1a. First, 1 g $C_6H_{12}O_6$ H_2O and 8.6 g NaCl were dissolved in 22 mL deionized (DI) water with the assistance of magnetic stirring, which was followed by adding 2 mL $CoCl_2$ aqueous solution (3 mg/mL). Then, the aqueous solution was frozen in liquid nitrogen, and the yielded solid was transferred to a freeze dryer. After 3 days of drying, a fluffy mixture containing $CoCl_2$-NaCl glucose was obtained. Afterwards, the $CoCl_2$-NaCl glucose was heated at 750 °C for 2 h under a gas flow of 150 sccm Ar and 50 sccm NH_3. The carbonized product was washed with DI water and dried in an oven at 60 °C for 12 h to obtain CoAT-NC. In addition, two control samples, nitrogen doped porous carbon (NC) and cobalt nanoparticle decorated nitrogen doped porous carbon (CoNP-NC), were prepared by applying 0 and 8 mL of $CoCl_2$, respectively, when preparing the aqueous solution.

The scanning electron microscopy (SEM) image in Fig. 1b demonstrates that CoAT-NC presents a honeycomb crosslinked porous structure. These honeycombs are formed by ultrathin carbon walls and have a pore size of 1–2 μm (Fig. 1c). The large pores can facilitate the electrolyte transport during the charge-discharge process [19–21]. These honeycombs are not observed from the SEM images of NC and CoNP-NC (Fig. S1 in Supporting information). Whereas, the X-ray diffraction patterns (XRD) and Raman spectra (Fig. S2 in Supporting information) of the NC, CoAT-NC, and CoNP-NC are similar and show typical features of amorphous carbon with very low graphitic level [22], which is in accordance with the low thermal treatment temperature applied in this work. The dispersion state of cobalt is further evaluated by transmission electron microscopy (TEM). The lattice fringes that can be assigned to the metallic cobalt or cobalt oxides nanoparticles are not observed in the bright field TEM image (Fig. 1d); the selected area electron diffraction (SAED) pattern captured in a circle area of 1 μm in diameter presents only halo rings (inset of Fig. 1d); and the image obtained from a spherical aberration corrected TEM present bright spots, which are Co atoms, uniformly disperse in the carbon film (Fig. 1e). In comparison, nanocrystals of CoO_x are observed in the TEM image obtained from the CoNP-NC (Fig. S3 in Supporting information). In addition, the morphology observed in the annular dark-field image matches well with the element maps of carbon, nitrogen, and cobalt (Figs. 1f–i), indicating a uniform element distribution in the carbon sheets. Based on these TEM analysis, the formation of cobalt atom doped carbon material can be concluded.

Spectroscopic studies were performed to analysis the chemical composition and the possible bonding configuration of the Co and N atoms in the graphene lattices. The X-ray photoelectron spectroscopy (XPS) survey spectra in Fig. 2a show that the NC, CoAT-NC, and CoNP-NC are composed of C, N and O elements, and Co is detected in the CoAT-NC and CoNP-NC. The content of the above elements measured by XPS is summarized in Table 1. A high N atom ratio of 12.6 at% is observed, which can improve the EDL capacitance by mediating the electronic conductivity and upper shifting the Fermi level of the carbon materials according to our previous research [17]. The atom concentrations of Co in the CoAT-NC and CoNP-NC are 0.14 and 0.60 at%, respectively, which are in agreement with that (0.15 at% for CoAT-NC and 0.60 at% for CoNP-NC) measured by inductively coupled plasma atomic emission spectrometer (ICP-AES) (Fig. 2b). Oxygen is observed in all of the three samples, and the C/O atom ratios are 18.2, 13.3 and 17.9 for

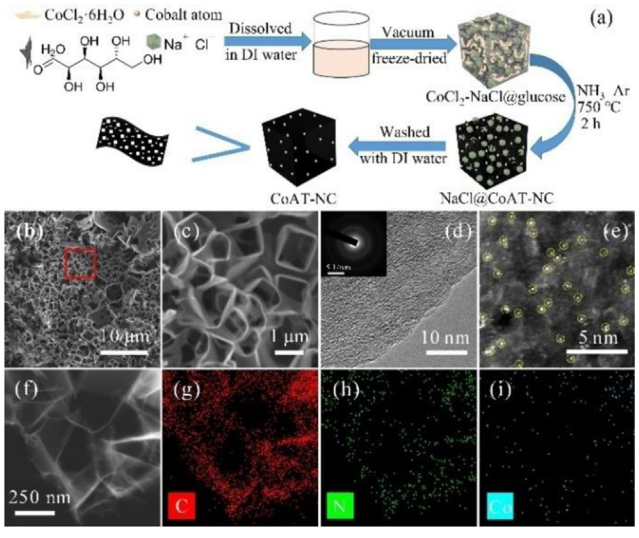

Fig. 1. (a) Schematic diagram of the synthesis process of CoAT-NC. (b, c) SEM images of CoAT-NC acquired. (d) high-magnification TEM images of CoAT-NC. Inset in (d) is the SAED pattern. (e) spherical aberration corrected TEM images of CoAT-NC. (f) TEM image and (g–i) the corresponding elemental mapping images of CoAT-NC.

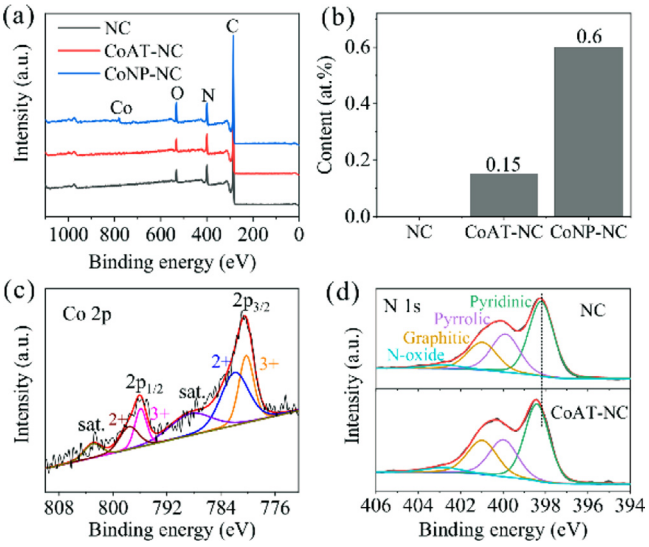

Fig. 2. (a) XPS survey spectra of the NC, CoAT-NC and CoNP-NC. (b) Atoms percentages of Co in the NC, CoAT-NC and CoNP-NC calculated by ICP-AES results. (c) High-resolution XPS Co 2p spectrum of CoAT-NC. (d) High-resolution XPS N 1s spectra of NC and CoAT-NC.

Table 1
Elemental composition and porous properties of the samples derived from glucose.

Samples	XPS (at%)				C/O	S_{BET} (m^2/g)	Porous properties (cm^3/g)		
	C	N	O	Co			V_p[a]	V_{micro}[b]	V_{meso}[b]
NC	82.7	12.6	4.62	0.00	17.9	710	0.38	0.31	0.06
CoAT-NC	83.1	12.1	4.57	0.14	18.2	870	0.73	0.32	0.32
CoNP-NC	80.7	12.6	6.05	0.60	13.3	831	0.59	0.32	0.21

[a]Pore volume, measured at $P/P_0 = 0.99$.
[b]Both micropore volume andmesopore volume are analyzed based on NLDFT.

the CoAT-NC, CoNP-NC and NC, respectively, indicating the effective reduction of the carbon-based materials through thermal annealing.

Fig. 2c shows the Co 2p XPS spectrum of CoAT-NC. Due to spin-orbit coupling, the Co 2p spectrum splits into two parts, $2p_{1/2}$ and $2p_{3/2}$. Characteristics of Co 2p can be assigned to Co^{2+} ($2p_{1/2}$, 797.6 eV and $2p_{3/2}$, 782.0 eV) and Co^{3+} ($2p_{1/2}$, 795.9 eV and $2p_{3/2}$, 780.6 eV), which are accompanied by two oscillating satellite peaks [23,24]. The energy difference between the peak positions of $2p_{1/2}$ (795.6 eV) and $2p_{3/2}$ (780.6 eV) is 15.0 eV, indicating that Co(III) mainly exists in the CoAT-NC [25,26]. The N 1s XPS spectrum of CoAT-NC is shown together with that of NC in Fig. 2d. Both the CoAT-NC and NC consist of pyridinic, pyrrolic, graphitic, and oxidized nitrogen. Note that the binding energy of pyridinic nitrogen in the CoAT-NC upper shifts by 0.3 eV comparing to that in the NC, which can be ascribed to the strong charge transfer from the pyridinic nitrogen to cobalt atom, indicating that cobalt atoms in the CoAT-NC mainly connect with pyridinic nitrogen [18]. Meanwhile, recent studies have also shown that nitrogen atoms are the coordination sites for transition metals in the nitrogen-doped carbon materials, which are widely used as electrocatalytic reactions [27–29].

The SSA and pore structure of the three samples were analyzed using nitrogen adsorption-desorption isotherms (Figs. S4a–c in Supporting information), from which the SSA calculated using Brunauer–Emmett–Teller (BET) theory are 710, 870 and 831 m^2/g for the NC, CoAT-NC and CoNP-NC, respectively. Nonlocal density functional theory (NLDFT) was applied to calculate the pore size distribution, and the results are shown in Fig. S4d (Supporting information). Large pores with pore width of 20–60 nm are observed in both of the CoAT-NC and CoNP-NC, while they are absent in the NC, indicating that the presence of cobalt during the thermal annealing process also creates large pores. These large pores can accommodate electrolyte and facilitate the ion transport during the charge-discharge process [30]. Whereas, the total surface area of both the CoAT-NC and CoNP-NC are majorly contributed by the micro- and mesopores (Table 1).

To assess the electrochemical properties of the materials, NC, CoAT-NC, and CoNP-NC were first coated on glassy carbon electrodes and measured in 1 mol/L H_2SO_4 in a three-electrode system (Fig. S5 in Supporting information). It is obvious that the cyclic voltammetry (CV) curves of the three samples acquired at different scan rates are all rectangular in shape, typical of the EDL capacitive behavior [31].

The electrochemical performance of the materials were further evaluated using two-electrode cells (see Supporting information). From the galvanostatic charge-discharge (GCD) curves of all the samples measured at 10 A/g (Fig. 3a) in 1 mol/L H_2SO_4, one can see that the CoAT-NC-based supercapacitor has a IR drop of only 2 mV, significantly smaller than those of the NC (7 mV) and CoNP-NC

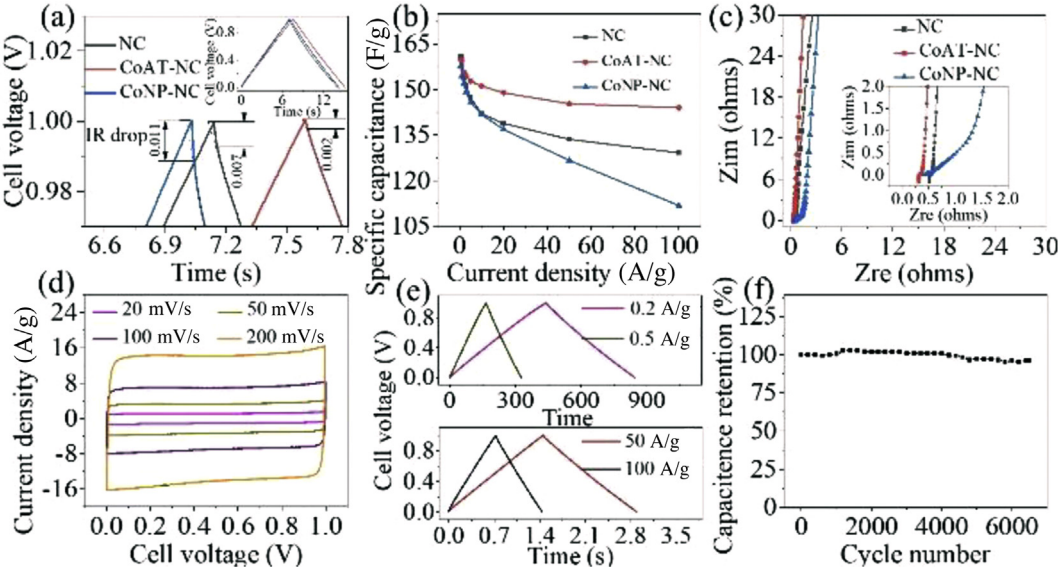

Fig. 3. EDL capacitor performance of samples measured in 1 mol/L H_2SO_4 aqueous electrolyte in a voltage range of 0–1 V using the two-electrode cells. (a) GCD curves of different samples measured at 10 A/g. (b) Comparison of the specific capacitances measured at various current densities. (c) Nyquist plots of the samples. (d) CV curves of CoAT-NC measured at scan rates of 20–200 mV/s. (e) GCD curves of CoAT-NC measured at different current densities of 0.2–100 A/g. (f) Cycling stability of CoAT-NC measured at 2 A/g.

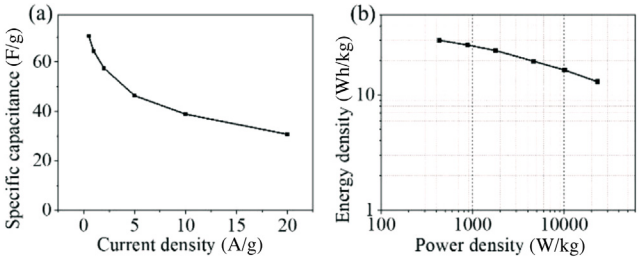

Fig. 4. (a) Gravimetric capacitances measured at different current densities and the (b) Ragone plot of CoAT-NC measured with a two-electrode cell using BMIM BF_4/AN as the electrolyte.

(11 mV). The negligible IR drop of the CoAT-NC, indicating excellent electrical conductivity of the CoAT-NC, which is critical for a supercapacitor to maintain a high capacitance at high charge-discharge current densities [32]. As expected, though the CoAT-NC, NC, and CoNP-NC output the similar specific capacitance of 160 F/g at 0.5 A/g in the acidic electrolyte, the CoAT-NC can retain a specific capacitance of 144 F/g at a very high current density of 100 A/g, considerably larger than those of the NC and CoNP-NC (Fig. 3b). This result is consistent with the low series and charge transfer resistances of the CoAT-NC measured by electrochemical impedance spectroscopy (EIS) (Fig. 3c) and the negligible voltage hysteresis revealed by the CV curves (Fig. 3d). Note that the GCD tests performed with the CoAT-NC at current densities of 0.2–100 A/g (Fig. 3e and Fig. S6a in Supporting information) show symmetric curves with negligible IR drop even at the high current density of 100 A/g, while that of CoNP-NC is distorted (Fig. S6b in Supporting information). The low IR drop in the GCD curves and the high capacitance retention of the CoAT-NC are also observed in 6 mol/L KOH from 0 to 1 V (Fig. S7 in Supporting information), which should be due to the improved electrical conductivity of CoAT-NC. Our previous research indicates that the Co-N moieties doped in the carbon matrix can considerably increase the DOS of the carbon based material [18], which renders a higher electrical conductivity and quantum capacitance [8,17]. It is reasonable to understand that the Co-N dopants and the associated change in the electronic structure of the carbon materials should be responsible for the improved electrochemical performance of the CoAT-NC observed in this work. Moreover, the better rate performance of CoAT-NC could be due to the unique honeycomb crosslinked porous structure, and the lack of faradaic reaction which is indicated by the rectangular shape of the CV profiles measured at high scan rates. Particularly, the CoAT-NC can maintain 96.3% of its original capacitance after cycling for 6500 times at 2 A/g in 1 mol/L H_2SO_4 aqueous electrolyte (Fig. 3f), indicating outstanding cycling stability.

Energy density is an important parameter for the supercapacitors. In order to evaluate the potential of the CoAT-NC as an electrode material for the supercapacitors, the capacitance behavior of CoAT-NC was also studied using BMIM BF_4/AN as the electrolyte in a two-electrode cell. Both the CV curves and the GCD curves (Fig. S8 in Supporting information) show typical EDL capacitive behavior in a voltage range of 0–3.5 V, which yield a specific capacitance of 70 F/g at 0.5 A/g (Fig. 4a). The calculated energy densities are 30 and 13 Wh/kg at the power densities of 0.4 and 23 kW/kg (Fig. 4b), respectively, based on the mass of the electrode material, which is promising for practical supercapacitors.

In summary, a porous carbon material doped with cobalt and nitrogen atoms is synthesized by carbonizing glycose at the presence of cobalt chloride under ammonia flow. Cobalt atoms connected with primarily pyridinic nitrogen atoms can uniformly dispersed in the amorphous carbon matrix, which is benefit for improving electrical conductivity and DOS of the carbon material. Electrochemical performance of the CoAT-NC measured in both the acidic and alkali aqueous electrolytes present good gravimetric capacitance of 160 F/g combing with outstanding capacitance retention of 90% at an extremely high current density of 100 A/g. A good energy density of 30 Wh/kg is achieved using organic based electrolyte. These results indicate that metal atom doping can be a promising way to optimize the electrochemical performance of the carbon based electrode materials for advanced supercapacitors.

Declaration of competing interest

The authors declare that they have no known competing financial interests or personal relationships that could have appeared to influence the work reported in this paper.

Acknowledgments

The authors are thankful for financial support from the National Natural Science Foundation of China (Nos. 51761145046, 51672262, 21503064), 100 Talents Program of the Chinese Academy of Sciences, National Program for Support of Topnotch Young Professional, and Fundamental Research Funds for the Central Universities (No. WK2060140003) and iChEM.

Appendix A. Supplementary data

Supplementary material related to this article can be found, in the online version, at doi:https://doi.org/10.1016/j.cclet.2020.04.058.

References

[1] D.Y. Qu, H. Shi, J. Power Sources 74 (1998) 99–107.
[2] T. Brezesinski, J. Wang, S.H. Tolbert, et al., Nat. Mater. 9 (2010) 146–151.
[3] P. Simon, Y. Gogotsi, Nat. Mater. 7 (2008) 845–854.
[4] Y. Gong, D. Li, C. Luo, et al., Green Chem. 19 (2017) 4132–4140.
[5] M. Yang, Z. Zhou, Adv. Sci. 4 (2017) 1600408.
[6] L.L. Zhang, X.S. Zhao, Chem. Soc. Rev. 38 (2009) 2520–2531.
[7] R. Chen, F. Wu, L. Li, et al., J. Phys. Chem. C 111 (2007) 5184–5194.
[8] H. Ji, X. Zhao, Z. Qiao, et al., Nat. Commun. 5 (2014) 3317.
[9] F. Beguin, V. Presser, A. Balducci, et al., Adv. Mater. 26 (2014) 2219–2251.
[10] L.L. Zhang, Y. Gu, X.S. Zhao, J. Mater. Chem. A 1 (2013) 9395–9408.
[11] L. Zhang, F. Zhang, X. Yang, et al., Sci. Rep. UK 3 (2013) 1408.
[12] J. Lee, J. Kim, T. Hyeon, Adv. Mater. 18 (2006) 2073–2094.
[13] Y. Xu, G. Shi, X. Duan, Acc. Chem. Res. 48 (2015) 1666–1675.
[14] X. Wang, Y. Zhang, C. Zhi, et al., Nat. Commun. 4 (2013) 2905.
[15] Y. Zhu, S. Murali, M.D. Stoller, et al., Science 332 (2011) 1537–1541.
[16] J. Chmiola, G. Yushin, Y. Gogotsi, et al., Science 313 (2006) 1760–1763.
[17] J. Chen, Y. Han, X. Kong, et al., Angew. Chem. Int. Ed. 55 (2016) 13822–13827.
[18] Z. Du, X. Chen, W. Hu, et al., J. Am. Chem. Soc. 141 (2019) 3977–3985.
[19] H. Tong, S. Yue, F. Jin, et al., Ceram. Int. 44 (2018) 3113–3121.
[20] W. Zhang, C. Xu, C. Ma, et al., Adv. Mater. 29 (2017) 1701677.
[21] M. Liu, J. Niu, Z. Zhang, et al., Nano Energy 51 (2018) 366–372.
[22] J. Xu, Z. Tan, W. Zeng, et al., Adv. Mater. 28 (2016) 5222–5228.
[23] Q.S. Huang, P.J. Zhou, H. Yang, et al., Electrochim. Acta 232 (2017) 339–347.
[24] Y. Liu, L. Yu, X. Jiang, et al., Int. J. Energy Res. 43 (2019) 4217–4228.
[25] H. Fei, J. Dong, M.J. Arellano-Jiménez, et al., Nat. Commun. 6 (2015) 8668.
[26] E.S. Andreiadis, P.-A. Jacques, P.D. Tran, et al., Nat. Chem. 5 (2013) 48–53.
[27] Y. Jiao, Y. Zheng, P. Chen, et al., J. Am. Chem. Soc. 139 (2017) 18093–18100.
[28] Y. Zheng, Y. Jiao, Y. Zhu, et al., J. Am. Chem. Soc. 139 (2017) 3336–3339.
[29] A. Wang, J. Li, T. Zhang, Int. Rev. Chem. Eng. 2 (2018) 65–81.
[30] T. Purkait, G. Singh, M. Singh, et al., Sci. Rep. UK 7 (2017) 15239.
[31] X. Sun, J. Ye, F. Pan, et al., New J. Chem. 42 (2018) 12421–12428.
[32] M. Sevilla, A.B. Fuertes, ACS Nano 8 (2014) 5069–5078.